Verlinde's emergent gravity vs MOND and the case of dwarf spheroidals

Alberto Diez-Tejedor,[1] Alma X. Gonzalez-Morales,[1,2] and Gustavo Niz[1]

[1] *Departamento de Física, División de Ciencias e Ingenierías, Campus León, Universidad de Guanajuato, 37150, León, México*

[2] *Consejo Nacional de Ciencia y Tecnología, Av. Insurgentes Sur 1582, Colonia Crédito Constructor, Del. Benito Jurez, 03940, México D.F. México*

In a recent paper, Erik Verlinde has further developed the interesting possibility that spacetime and gravity may emerge from the entanglement structure of an underlying microscopic theory. In this picture dark matter arises as the response to the standard model of particle physics from the delocalized low energy degrees of freedom that build up the dark energy component of the Universe. Physics is then regulated by a characteristic acceleration scale a_0, identified in this model with the dark energy de Sitter radius by $a_0 = cH_0 \approx 5.4 \times 10^{-10}\,\mathrm{m/s^2}$ (using *Planck* data). For a point particle, or outside an extended spherically symmetric massive object, Milgrom's empirical fitting formula is recovered. However, Verlinde's theory critically departs from MOND when considering the inner structure of galaxies. For illustration, we use the the eight classical dwarf spheroidal satellites of the Milky Way. These objects are perfect testbeds for the model given their spherical symmetry, measured kinematics, and large identified missing mass. As a consistency check we show that, for reasonable stellar mass-to-light ratios, Verlinde's theory can fit the velocity dispersion profile in dwarf spheroidals with no further need of an extra dark particle component. Finally we compare our results with the recent phenomenological interpolating MOND function of McGaugh *et al*, and find a departure of up to 50 percent in the innermost region of these galaxies.

PACS numbers: 95.35.+d, 98.80.Jk, 04.50.Kd, 98.56.Wm

arXiv:1612.06282v1 [astro-ph.CO] 19 Dec 2016

I. INTRODUCTION AND SUMMARY OF RESULTS

The dark matter (DM) problem remains one of the big puzzles in modern cosmology [1]. It is commonly accepted that this component consists on a new particle, not included in the standard model sector. It is expected to interact so weakly with the visible matter that, at present, it has not been possible to detect this particle in accelerators, nor through direct or indirect astrophysical probes (see however [2] for positive claimed signals). It is noteworthy, however, that all solid evidence pointing to the existence of this mysterious component comes from observations that involve the gravitational interaction in some way or another. Therefore, it has also been considered that the mass discrepancy suggesting the existence of DM may be the consequence of a poor understanding of gravity at large scales.

Following this line of thought, Mordehai Milgrom, in a series of seminal papers published in the Astrophysical Journal in 1983 [3], proposed the original idea that the missing mass problem in galaxies could be resolved by a modification of Newton's law in the extremely weak field regime. In practice, this modified Newtonian dynamics (MOND) can be implemented in many different ways [4]. Here we use a non-conventional parametrization in terms of a phenomenological interpolating function ζ defined in such a way that it relates the effective or observed gravitational field g, to the standard Newtonian expression $g_B = GM_B/r^2$, namely

$$g = \zeta(g_B/a_M)g_B\,. \tag{1}$$

Here $M_B(r)$ denotes the mass distribution in the object, and the subscript B in the different quantities stresses that there are only baryons (in the cosmological acceptance of the word) in the configuration. Notice that there is only one free parameter in the model, a characteristic acceleration scale a_M, to be determined empirically. In our parametrization the interpolating function ζ depends on $y \equiv g_B/a_M$ only. In order to reproduce Solar System observations we need that $\zeta(y \gg 1) = 1$, thus $g = g_B$. If we assume further that $\zeta(y \ll 1) = 1/\sqrt{y}$, the gravitational interaction will change from the usual $g = g_B$ in the Earth's laboratories, to the famous Milgrom's fitting formula $g = \sqrt{a_M g_B}$ in the extremely weak field regime, $g_B \ll a_M$.

It has been extensively argued in the literature that this simple modification of the gravitational interaction can reproduce the flattening of the rotational curves as well as the baryonic Tully-Fisher relation in spiral galaxies without postulating the existence of any new exotic matter component [4]. Apart form the two conditions above, the function $\zeta(y)$ was not fully characterized in the original theory. However, in a recent paper [5], using more than 2500 data points in 153 rotationally supported galaxies of different morphologies and gas fractions, the authors found a correlation between the observed and baryonic accelerations that can be interpreted in terms of an interpolating MOND formula of the form

$$\zeta_{\mathrm{McGaugh}}(y) = \frac{1}{1-\exp(-\sqrt{y})}\,, \tag{2}$$

with the characteristic acceleration found to be $a_M = 1.20 \pm 0.26 \times 10^{-10}\,\mathrm{m/s^2}$. Naturally this function $\zeta_{\mathrm{McGaugh}}(y)$ satisfies the two limiting conditions stated above for $y \gg 1$ and $y \ll 1$.

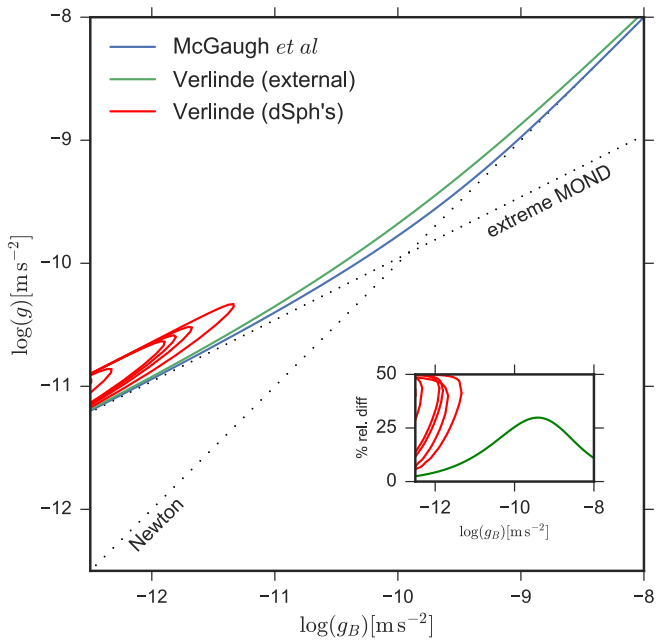

FIG. 1: *Blue line:* Empirical correlation between the baryonic acceleration, g_B, and the actual one, g, as reported by McGaugh *et al* [5]. *Green line:* The prediction of Verlinde's theory outside a spherically symmetric massive object. Note that at intermediate acceleration scales Verlinde's model is marginally consistent with respect the 20 percent observational uncertainty of the McGaugh interpolating function, while both tend to the same limiting behavior for large and small accelerations. *Red lines:* Predicted correlation for the classical eight dSph satellites of the Milky Way within the Verlinde's framework. Here we have adopted a Plummer profile for the distribution of baryons in these objects, and used $a_0 = 5.4 \times 10^{-10}\,\mathrm{m/s^2}$ and the data in Table I. Note that the correlation between the two accelerations g and g_B depends in general on how baryons are distributed in the configuration; a detailed description of this is shown in Figure 2. For reference we have added the corresponding correlation for the extreme MOND (Milgrom's formula), and Newton, regimes.

Even if Milgrom's modified Newtonian dynamics provides a satisfactory phenomenological description of the galactic kinematics, it presents some difficulties when trying to describe objects at different scales. For instance, galaxy observations suggest that $a_M \approx 1.2 \times 10^{-10}\,\mathrm{m/s^2}$, consistent with the value reported in [5], whereas observations in galaxy clusters point to a value that differs by a factor of three or four [6], and strong lensing in big galaxies to an even larger value [4]. These discrepancies may just signal that one should look at Milgrom's fitting formula as an effective description in the appropriate regime, expecting that the underlying modified gravity theory will explain DM beyond the validity of MOND.

Furthermore, there is an intriguing relation in this phenomenological model, where the characteristic acceleration scale used to explain the rotational curves in galaxies seems to be controlled by the value of the Hubble constant today [7]. The link between dark energy (DE) and DM may be a hint for an emergent phenomenon of the underlying bricks of spacetime. Motivated by all these arguments, Erik Verlinde has recently proposed that the emergent laws of gravity may contain an additional *dark* gravitational term that could replace DM in galaxy observations [8]. Then, what we use to identify as DM could be just the inescapable consequence of the presence of standard model particles in those objects.

The main result of this work is summarized in Figure 1, where we show how the emergent gravity theory proposed by Verlinde in Ref. [8] departs from the successful phenomenological MOND prescription, and in particular from the recently proposed interpolating function of McGaugh *et al* [5]. The main plot relates the observed or effective gravitational field g, to the standard Newtonian one g_B inferred from the baryonic (stellar and gas) mass distribution. The blue line in Figure 1 denotes the fit to the observational data of McGaugh *et al* based on the interpolating function in Eq. (2), whereas the green one the prediction of the Verlinde's model for the exterior of a spherically symmetric galaxy. Both descriptions agree at large and small accelerations, i.e. in the Newtonian and extreme MOND regimes, as expected. However, in the intermediate region they differ up to 30 percent, though this difference is still consistent with the observational uncertainties of the empirical relation in Eq. (2).

When it comes to the interior of galaxies, MOND-like theories (and then also the empirical relationship of McGaugh *et al*) do not change their behavior, staying along their corresponding lines of Figure 1. However, for Verlinde's model the observed acceleration depends on gradients of the baryonic distribution of matter, increasing the observed gravitational field g with respect the extreme MOND regime. In red lines one could appreciate the prediction of Verlinde's emergent gravity model for the classical eight dwarf spheroidal (dSph) galaxies of the Milky Way, resulting in a 50 percent deviation from MOND well inside the galaxies. The details of the results, and more implications, are discussed along the present work.

The paper is organized as follows. In Section II we outline the general picture developed by Verlinde in Ref. [8]. The reader not interested in the technical details that motivate this proposal, or that is familiarized with Verlinde's work, can skip this section. In Section III we compare Verlinde's model with the successful phenomenological MOND description, and then argue in Section IV that the new theory can fit the velocity dispersions of the eight classical dSph's satellites of the Milky Way with no further need of an extra dark particle component. We finally present, in Section V, a brief discussion on the results.

II. VERLINDE'S EMERGENT GRAVITY PROPOSAL

On one hand, classical general relativity is a well developed area of physics. However, we still lack a fully quantum description of this theory. On the other hand, emergent phenomena —which has a vague definition in the literature— occur in physical and other natural sciences all the time. The appearance of thermodynamics and hydrodynamics from microscopic states are probably the two notorious cases in physics, but there are many other well known examples that illustrates this situation, such as the Van der Waals force emerging from non-relativistic quantum electrodynamics [9], or the laws of classical mechanics from quantum theory when applied to large enough systems. Among these ideas to understand gravity at the quantum level, one may wonder whether the laws of gravity, and perhaps even the structure of spacetime itself, unfold somehow as a collective result of some unknown microscopic degrees of freedom.

This is no longer a new idea. Early work dates back to more than fifty years ago with the proposals of Wheeler, Finkelstein or Sakharov [10, 11], becoming more popular in the last decade with particular connections to the concepts of entropy, entanglement, and the gauge/gravity duality. This duality, in simple words, states that a field theory without gravity is equivalent to a higher dimensional theory containing gravity, supporting the idea of the gravitational field as an emergent concept. We refer the reader to the review papers in [12, 13] and references within, where different approaches, challenges, and problems of emergent gravity are described in some detail.

Among the vast constructions of emergent gravity, which usually break Lorentz invariance at the microscopic level [12, 14], there is one exception started by the work of Ted Jacobson in Ref. [15]. In that work, he showed how Einstein equations can be recovered from the black hole entropy and the standard concepts of heat, entropy, and temperature in thermodynamics. Given that thermodynamics reflects the collective behavior of microstates, this particular perspective of gravity as an entropic force further supports the idea of an emergent spacetime. This early work was then further explored and generalized by Thanu Padmanabhan (see [16] and references therein) and Verlinde [17], highlighting the deep connection between general relativity and entropy. A key argument in this relationship is the "area law" scaling of entropy, as opposed to the usual volume scaling. At the microscopic level, it is well understood that local interactions with a gapped Hamiltonian lead to an area law for the entanglement entropy [18], connecting ideas in black holes (and thus gravity), information theory, and quantum many body physics.

Motivated by all these arguments, Verlinde [8] has again extended this thermodynamical picture to explain the dark sector, *c'est-à-dire* the DM and DE in our Universe. In the new proposal he sketches, without rigorous proofs, how the quasi-de Sitter (dS) spacetime in which we live at the moment (the DE domination phase), can be obtained from a not well-specified system of microstates which are coherently excited above the true vacuum. This ground state, corresponding to a negative cosmological constant anti-de Sitter (AdS) spacetime, emerges out of the microstates which are fully entangled. This particular construction could be better understood in terms of a representation of the microstates called the Multiscale Entanglement Renormalization Ansatz (MERA) tensor network within the gauge/gravity correspondence.

A tensor network uses sites and connections to mathematically reduce the problem of finding the (vacuum) state in a system of many quantum particles. Using a coarse graining algorithm one can systematically reduce the number of degrees of freedom at each level. Then, after repeating it iteratively, one obtains a network. This mathematical description of many body physics has turned out to be very effective in studying condensed matter systems, and has the interesting property of developing an effective metric along the network in many cases [19]. In the case of the gauge/gravity duality, out of the possible tensor network descriptions, the particular choice of MERA develops an effective metric which results in a pure AdS when the continuum limit is taken [20].

An important result is how the area law is obtained along this construction. The microstates are fully locally entangled, so that one can push the relevant information of the tensor network to the boundary of AdS. The relevant degrees of freedom to describe the full network are then those which live in the boundary of a lower dimensional space, which correspond precisely to the field theory in the duality [21]. Therefore, one does expect that the microstates (perhaps of this MERA tensor network) are the building blocks behind the AdS ground state.

From the AdS ground state, Verlinde argues that one could obtain a dS space (a vacuum spacetime with the DE component only), as an excited state over this vacuum with very particular properties. One may expect a thermalized state due to the fact that dS has a horizon, and hence a Bekenstein's temperature associated to it. In order to achieve this homogeneous, very low energetic excited state, one may argue for long range correlations among the microstates, and hence not an area law but a volume scaling entropy. This volume scaling entropy precisely matches the area law at the cosmological horizon, implying the entropy of DE within a spherical region of radius r is

$$S_{DE} = \frac{r}{L}\frac{A(r)}{4G\hbar}\,. \tag{3}$$

Here L is the Hubble scale, related to the Hubble constant by $H_0 = c/L$, and $A(r)$ is the area enclosing the spherical region. The DE entropy should then be distributed equally among all the states, so that the excitations are delocalized and with a very slow dynamics, inhibiting all possible observation of DE in the lab. One may think that these non-local excitations that construct

dS spacetime produce a very stiff structure, but on the contrary the slow dynamics of these states makes it resemble more of an elastic medium. Verlinde uses the theory of elasticity to get predictions, since at the moment there is no clear understanding of the real microstates describing the system.

The idea of gravity being thought in terms of elasticity dates back to the work of Sakharov [11], and more recently the possibility of describing dS in terms of an elastic medium was also worked out by Padmanabhan in Ref. [22], where he even argues how to obtain the value of the observed cosmological constant from this description. However, the real novelty in Verlinde's work is the study of how this dS scheme is affected by the intrusion of a baryonic mass M_B. On one hand, the cosmological horizon shrinks by the presence of the mass, reducing the entropy associated to the DE, as one can easily get convinced from the Schwarszchild-de-Sitter solution if the mass is placed near the origin at $r = 0$ in the static patch of dS. On the other hand, this mass will carry a volume-scaling entropy given by $|S_M| = (2\pi M r)/\hbar$, as it can be shown by the effect of the gravitational potential produced by the mass in the geodesic distance. If we then compare this mass entropy to the entropy lost by the medium by the presence of the mass we get

$$\epsilon(r) \equiv \frac{8\pi G}{a_0}\Sigma_B(r) \lesseqgtr 1\,, \tag{4}$$

where $\Sigma_B \equiv M_B/A(r)$ is the surface density and we have introduced the characteristic acceleration a_0 of the DE, given by $a_0 = c\,H_0$. If $\epsilon > 1$, more entropy is removed by the mass and the response to it is governed by the usual laws of Einstein's theory without dark fluids. If the opposite is true, $\epsilon < 1$, then we are in the low surface density regime and there is a remnant of the DE entropy in the volume occupied by the mass, which behaves as an incompressible elastic medium and will affect the gravitational laws associated to the baryonic mass, mimicking DM.

It turns out that ϵ corresponds to the largest principle of the elastic medium strain, namely $(\epsilon_{ij} - \epsilon_{kk}\delta_{ij})n_j = \epsilon n_i$, where is ϵ_{ij} is the strain tensor and n_i is the maximal strain (unitary) direction. Therefore, the response of the medium to the mass inclusion can be fully understood in terms of the stress and the strain of the elastic theory. The elastic linear theory considered by Verlinde [8] is such that no pressure waves are present and the displacement is produced by a scalar quantity only, namely, the stress tensor σ_{ij} obeys $\sigma_{ij} = a_0^2(\epsilon_{ij} - \epsilon_{kk}\delta_{ij})/(8\pi G)$. This corresponds to a theory of gravity with a central force, described by a scalar potential Φ in terms of the elastic medium displacement u_i, and given by $\Phi = a_0 u_i n_i$.

In order to obtain the main result of Ref. [8], Eq. (4) can be though in a different way. If we are in the dark sector regime, $\epsilon < 1$, the observed surface density produced by baryons is given by $\Sigma_D \equiv a_0\epsilon/8\pi G$. From the entropy removed by considering the mass M_B inclusion, Verlinde arrives to the key equation

$$\left(\frac{8\pi G}{a_0}\Sigma_D\right)^2 \leq \frac{1}{2}\nabla_i\left(\frac{\Phi_B}{a_0}n_i\right)\,, \tag{5}$$

where the equality is only achieved when the largest principle strain ϵ takes its maximal value (so the perpendicular strains are all equal), and the medium response is negligible well outside the mass. In other words, observations may only put a lower bound on the parameter a_0, since a larger value can be accommodated by having a smaller elongation (or compression) of the elastic medium due to the baryonic mass inclusion.

In the case of a maximal value for the largest principal strain, and assuming further spherical symmetry, we have that $\Sigma_B = -\Phi_B/(4\pi G\, r) = M(r)/A(r)$, where $M(r) = \int_0^r \nu(y)A(y)dy$, and the previous key formula in Eq. (5) reduces to our starting point for the analysis in this paper,

$$M_D^2(r) = \frac{a_0 r^2}{6G}\frac{d}{dr}\left(rM_B(r)\right)\,. \tag{6}$$

As stated earlier, the parameter $a_0 = cH_0$ is a characteristic acceleration scale in the theory related to the radius of the (quasi)-dS universe we seem to inhabit, H_0. Using current cosmological observations we obtain $a_0 = 5.4 \times 10^{-10}\,\mathrm{m/s^2}$ [23].

III. VERLINDE'S EMERGENT GRAVITY VS MOND

Baryons and the DM phenomena are highly correlated in this new gravitational picture, and this is a prediction that must be contrasted against observations. For a point particle, or outside and extended massive object, $M_B(r) = \text{const.}$, which translates to $M_D^2(r) = a_0 M_B r^2/6G$ from Eq. (6). In the extremely weak field regime, $g_B \ll a_0$, we recover Milgrom's original fitting formula $g(r) = \sqrt{a_M g_B(r)}$, where $g_B = GM_B/r^2$. Note that the factor $a_M = a_0/6$ is now related in an obvious way to cosmological quantities. This seems to suggest that one can explain the kinematics of spiral galaxies as well as MOND can do, although that is not really true at this level, since the derivation of Eq. (6) was based on spherical symmetry, which is not fulfilled by baryons in those objects. Furthermore, Milgrom's fitting formula is only recovered in the exterior of a massive object, but the new fitting formula differs inside matter distributions, as we discuss in detail in what follows. We should then test the viability of this new expression using astrophysical observations which are in agreement with the hypothesis of the derivation. For recent work on the observability of Verlinde's model see Refs. [24].

One may wonder how Verlinde's model differs from MOND for spherical objects. At this point it is interesting to stress that, for the emergent gravity model outlined

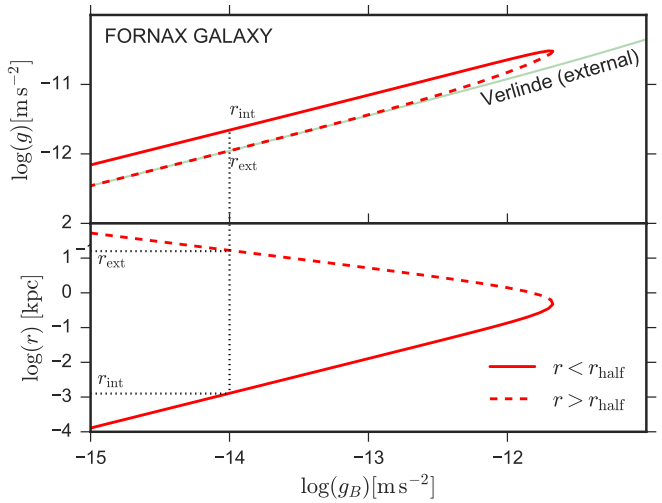

FIG. 2: Detailed behavior of the observed acceleration as a function of the baryonic component within Verlinde's theoretical framework. This relation depends on whether we are exploring an inner or an outer galactic region, as shown by the same baryonic acceleration at two different radii, $r_{\rm ext}$ and $r_{\rm int}$. The characteristic radius that separates the inner and outer regions is close to the half-light radius, but they do not coincide exactly. We have used a Plummer density profile to model the stellar mass distribution, and the structural parameters reported in Table I. The maximum difference with respect to the external profile is of about 50 percent, and it seems independent of the galaxy's details, see Figure 1. This inner region behavior is expected in general, since the acceleration in Verlinde's theory depends on the derivatives of the baryonic mass profile (see the text for a detailed explanation).

in Section II, it is still possible to relate the baryonic acceleration, g_B, to the actual observed one, g, through an interpolating function of the form

$$\zeta_{\rm Verlinde}(y, y') = 1 + \sqrt{\frac{3y + ry'}{6y^2}}\,. \qquad (7)$$

Contrary to what happens in the case of MOND, see Eq. (1) for reference, this function depends not only on $y = g_B/a_0$, but also on its radial derivative, $y' = dy/dr$. This derivative dependence of the interpolating function is expected to hold away from spherical symmetry, as one may appreciate from the general expression in Eq. (5), and it represents the stronger deviation from the MOND paradigm. This effect has already been pointed out by Verlinde [8], where he argues that the slope of a density profile can explain the orders of magnitude in cluster observations, or even how weak lensing systems could be affected, see also the work in Refs. [24]. In this paper we explore the inner part of galaxies in more detail, and in particular for those which are almost spherical in symmetry.

Outside an extended spherically symmetric massive object we have that $ry' = -2y$, hence an effective MOND-like regime with $\zeta^{\rm out}_{\rm Verlinde}(y) = 1 + 1/\sqrt{6y}$ naturally emerges as a particular limit of the full Verlinde's theory when matter distribution plays no significant role. Note the two limiting cases corresponding to the Newtonian, $\zeta^{\rm out}_{\rm Verlinde}(y \gg 1) = 1$, and the extreme MOND, $\zeta^{\rm out}_{\rm Verlinde}(y \gg 1) = 1/\sqrt{y_M}$, regimes that appear in the exterior region once we identify $y_M = 6y$, i.e. $a_M = a_0/6$.

While still considering the exterior of a massive object, one may wonder how the interpolating function in Eq. (2) compares to the Verlinde's model away from the extreme MOND regime. In Figure 1 we show the correlation bewteen the two acceleration profiles g and g_B, using the same scales as in Figure 3 of Ref. [5]. The blue line shows the result of the analysis carried out by McGaugh *et al*, a fit provided by 2693 data points in 153 rotationally supported objects of the SPARC database [5]. The green line corresponds to the MOND-like regime that emerges outside the exterior of a spherically symmetric massive object in Verlinde's theory. Note that the relative error between these two different models is never larger than 30 percent, marginally accepted by the observations, and both descriptions coincide in the Newtonian and the extreme MOND limits, as previously stated.

On the contrary, for the interior region of the object, the dependence of the interpolating function on y' implies there are no expressions independent of the density profile. In other words, the relation between g and g_B depends in general on the Newtonian potential profile, and then on how baryons are distributed in the configuration. It is important to stress that this feature makes it possible to distinguish, at least in principle, Verlinde's emergent gravity from MOND when using peculiar velocities in the inner galactic regions.

In MOND, the interior and the exterior regions describe the same acceleration profile, see blue and green lines in Figure 1. However, the radial derivative dependence of the interpolating function in Verlinde's model gets the interior profile of g to depart drastically from the outer region. To describe in detail the difference, one must select a particular configuration model. One of particular interest is the Plummer density profile [36], since it has been extensively used in the literature to describe (nearly) spherically symmetric stellar structures such as globular clusters, galactic bulges, and dSph galaxies. Current observation seem to indicate that the former examples are almost free of DM, while the latter ones are expected to be dominated by this component, hence our interest in dSph's as a probe of Verlinde's model.

The Plummer mass density profile is given by

$$\nu(r) = \frac{3\Upsilon_* L}{4\pi r_{\rm half}^3}\,\frac{1}{[1 + (r/r_{\rm half})^2]^{5/2}}\,, \qquad (8)$$

where L is the luminosity of the object and $r_{\rm half}$ is the half-light radius, the radius enclosing half of the total luminosity. We give more details about this profile and the dSph's in the following section, for the moment we just consider it as an example to explain the behavior of the acceleration in the inner and outer regions and its relation to the baryonic acceleration for an extended stellar configuration. This is illustrated in Figure 2 for the particu-

lar case of one dSph, Fornax. A turning point is precisely the expected behavior for a g vs g_B diagram, where an up-then-down density profile always leads to a forward-then-backwards acceleration function. Verlinde's model is different to MOND since the derivative moves the turning point away from the outer region behavior. The discrepancy between models in the interior field rises to 50 percent for the Plummer profile well inside the galaxies. This behavior is quite generic, the red lines in Figure 1 show the prediction for the eight classical dSph satellites of the Milky Way, were we have set the galaxy details according to our results in Section IV.

IV. MILKY WAY'S DWARF SPHEROIDALS IN THE EMERGENT GRAVITY PICTURE

Given the current degree of development of the theory, and until we can generalize the expression in Eq. (6) to configurations with less symmetry, nearby dSph galaxies are probably one of the most promising objects to test Verlinde's new proposal. These galaxies are the smallest and least luminous in the local group, and given their proximity they are relatively well understood. Stellar population studies point to a negligible gas contribution and stellar mass-to-light ratios in the range $1 \lesssim \Upsilon_* \lesssim 3$ [25]. However, there is evidence that they may require an absolute (not only stellar) mass-to-light ratio as large as $\Upsilon \sim 10 - 10^2$ in order to explain their internal kinematics [26]. The key point is that these systems reach the regime where standard Newtonian theory fails, and where we expect the heart of Verlinde's proposal to reveal.

The Plummer density profile in Eq. (8) provides a good description of the eight classical dSph satellites of the Milky Way, except maybe for two of them, Fornax and Leo, because apparently those do not exhibits signs of suffered stellar tidal stripping [29]. We can read their structural parameters values from Tables 4 and 5 of Ref. [30], and for convenience we also show them in our Table I.

Internal coherent rotation in dSph's is negligible, and the stellar component is supported against gravity by its random motion. Contrary to the case of spiral galaxies, the observation that can be used is not a rotation curve but, rather, the line-of-sight velocity dispersion of its components. In particular, in this work we use the data for the internal dynamics of the eight classical dSph satellites of the Milky Way, as reported in Walker *et al* [27, 28]. We assume, as usual, that each galaxy is spherically symmetric and in dynamical equilibrium (two assumption in Verlinde's derivation), with the stars tracing the underlying gravitational potential; in this case determined by the effective mass formula $M(r) = M_B(r) + M_D(r)$.

An analysis of the velocity dispersion profiles shows that the quantity that is best constrained is the enclosed mass at the half-light radius, $r = r_{\rm half}$ [28]. Therefore, to qualitatively compare MOND and Verlinde's models we have searched for the coefficient factor that the MOND's mass-to-light ratio needs to be scaled so that it matches Verlinde's profile at the half mass radius: $\Upsilon_*^{\rm M} = 5/2\Upsilon_*$, see Appendix A for details. This simple result means MOND may require a mass-to-Light ratio almost twice larger than Verlinde's theory for the same value of a_0. It is important to mention that stellar mass-to-light ratios in these dSph's are unknown. A study based on stellar formation histories (and independent from kinematics) finds a mean value of $\Upsilon_* = 1.03$ [34] (also a mean of $\Upsilon_* = 1.6$ was previously found in [35]). In general, it seems that stellar population studies point to values not much larger than unity [25], which may suggest Verlinde's model is favored along this line of thought. However, a detailed analysis of Verlinde's model should be taken using each dSph's data, which is the goal of the rest of this section.

In order to do a more quantitative analysis of the Verlinde's model and how well it describes dSph's kinematics, we perform a standard parametric Jeans analysis [27] (see Section 4.8 in Ref. [31] for a comprehensive review of these techniques. The (observed) line-of-sight velocity dispersion of the dSph's, $\sigma^2_{\rm los}(R)$, can be related to the (modelled) mass profile, $M(r)$, and stellar mass density, $\nu(R)$, through

$$\sigma^2_{\rm los}(R) \;=\; \frac{2G}{I(R)} \int_R^\infty dr' \nu(r') M(r') (r')^{2\beta-2} \times \int_R^{r'} dr \left(1 - \beta \frac{R^2}{r^2}\right) \frac{r^{-2\beta+1}}{\sqrt{r^2 - R^2}}\,, \qquad (9)$$

where R is the projected radius, and $\beta(r)$ represents the orbital anisotropy. This anisotropy is not constrained observationally and, in general, it is a function of the radius. However, as it is customary, we assume it to be constant in this work. The stellar mass density profile in Eq. (8) is recovered from the (observed) 2-dimensional, i.e. projected along the line-of-sight, stellar density $I(R)$,

$$I(R) = \frac{L}{\pi r^2_{\rm half}} \frac{1}{[1 + (R/r_{\rm half})^2]^2}\,. \qquad (10)$$

In order to fit the observational data we have three free parameters per galaxy: one associated with the theory, the acceleration scale a_0, and two associated with the stellar component, the stellar mass-to-light ratio Υ_*, and the orbital anisotropy β. Note that this is different from a standard DM particle halo where the mass-to-light ratio is uncorrelated to the DM density profile, and it actually cancels out in Eq. (9). To proceed further, we perform a Markov Chain Monte Carlo (MCMC) analysis to explore the parameter space and estimate the most probable value of the different quantities (we use the EMCEE code, described in Ref. [32]). Since the acceleration scale is a constant in the theory, one should perform a joint analysis for the eight galaxies keeping a_0 fixed. However, as we mentioned earlier, the parameter a_0 may be thought as encoding the hidden information about the

Object	L_V	$r_{\rm half}$	$\langle\sigma_{\rm los}\rangle$	Test 1 ($a_0 = a_{0,\rm theory}$)			Test 2 (a_0 unspecified)		
				Υ_*	β	$g/g_{\rm MW}$	a_0	Υ_*	β
	$(L_{V,\odot})$	(pc)	$(\mathrm{km\,s^{-1}})$	$(M_\odot\, L_{V,\odot}^{-1})$			$(\mathrm{m\,s^{-2}})$	$(M_\odot\, L_{V,\odot}^{-1})$	
Fornax	2.0×10^7	710 ± 77	11.7 ± 0.9	0.32	-0.15	0.15	1.9×10^{-9}	3.11	-0.17
Sculptor	2.3×10^6	283 ± 45	9.2 ± 1.1	1.58	-1	0.06	1.4×10^{-9}	0.64	-1
Carina	3.8×10^5	250 ± 39	6.6 ± 1.2	2.23	-0.97	0.07	1.2×10^{-9}	1.05	-0.98
Draco	2.9×10^5	221 ± 19	9.1 ± 1.2	13.08	<-1.5	0.04	3.1×10^{-9}	2.7	<-1.2
Leo I	5.5×10^6	251 ± 27	9.2 ± 1.4	8.69	-1	0.004	2.2×10^{-9}	2.44	-1.08
Leo II	7.4×10^5	176 ± 42	6.6 ± 0.7	2.38	0.13	0.01	8.6×10^{-10}	1.54	0.12
Sextans	4.4×10^5	695 ± 44	7.9 ± 1.3	2.09	-0.21	0.63	9.5×10^{-10}	1.21	-0.2
Ursa Minor	2.9×10^5	181 ± 27	9.5 ± 1.2	11.31	-1.8	0.03	2.7×10^{-9}	2.7	-1.8

TABLE I: Luminosity in the V-band L_V, half-light radius $r_{\rm half}$, and mean velocities $\langle\sigma_{\rm los}\rangle$, for the different objects as reported in Refs [30]. *Test 1:* Median values of the marginalized posterior distribution for the stellar mass-to-light ratio Υ_*, and orbital anisotropy β, taking the acceleration scale fixed to the theoretical value, $a_0 = 5.4\times10^{-10}\,\mathrm{m/s^2}$. *Test 2:* Median values of the marginalized posterior distribution for the acceleration scale a_0, stellar mass-to-light ratio Υ_*, and orbital anisotropy β. The theoretical value of a_0 is consistent at 2-σ level for all galaxies, and the fit to Fornax exhibits a bimodality for the stellar mass-to-light ratio, but is consistent with $\Upsilon_* < 6$, see Figure 4. Moreover, this strong degeneracy between a_0 and Υ_* may drive Υ_* to a lower, observationally accepted value at the cost of increasing a_0, which is consistent with not knowing the actual deformation profile of the elastic background medium. Note that the values of β in both tests are consistent, pointing to no degeneracy with other parameters.

elastic medium deformation if the principal strain does not take its maximal value, as it was assumed when taken the equality in Eq. (5) to deduce the expression in Eq. (6). Therefore, we perform two different tests that, steep by steep, help us to better understand the behavior of the model when trying to fit the internal kinematics of the eight classical dSphs:

Test 1: Fix the value of the acceleration scale to the prediction of the theory, $a_0 = 5.4\times10^{-10}\,\mathrm{m/s^2}$ [23], and find the most probable values of the orbital anisotropy β, and stellar mass-to-light ratio Υ_*, compatible with the data in each individual object. For this test we assume uniform priors in the range

$$-2 < \ln(\Upsilon_*[\Upsilon_\odot]) < 5\,, \tag{11a}$$
$$-3 < -\ln(1-\beta) < 3\,. \tag{11b}$$

The main purpose here is to determine if the theory, as it is, needs to include any extra DM, assuming the rest of Verlinde's hypotheses to get Eq. (6) are satisfied. The results of this test are summarized in Table I. Note that within this test, there is some tension between the observationally allowed range of values for the stellar mass-to-light ratios, in particular with that of Draco, $\Upsilon_* = 13.08$, and Ursa Minor, $\Upsilon_* = 11.31$. Furthermore, the value of the mass-to-light ratio for Fornax is quite low as well, $\Upsilon_* = 0.32$. In Figure 3 we show for illustration the posterior distribution of both parameters, the anisotropy and mass-to-light-ratio, for Fornax and Sculptor. Note they are well constrained and show no degeneracies.

Test 2: Find the most probable values of the acceleration scale a_0, orbital anisotropy β, and stellar mass-to-light ratio Υ_*, compatible with the data in each individual object. In this case, we adopt uniform priors in the range

$$-12 < \log(a_0[\mathrm{m\,s^{-2}}]) < -8\,, \tag{12a}$$
$$-2 < \ln(\Upsilon_*[\Upsilon_\odot]) < 5\,, \tag{12b}$$
$$-3 < -\ln(1-\beta) < 3\,. \tag{12c}$$

We determine the most likely value of Υ_* for each galaxy, marginalizing over a_0 and β, and check if it is within the range of acceptable values (i.e. no extra DM required), meanwhile the acceleration parameter is close (although not necessarily equal) to the theoretical one.

Again the results are shown in table I. Note that relaxing the value of a_0 improves the stellar mass-to-light ratios found, and that the values of β in both tests are consistent, pointing to no degeneracy with other parameters. As an example, we show in Figure 4 the posterior distribution of the three parameters (the acceleration scale, the anisotropy, and the stellar mass-to-light ratio) for Fornax and Sculpture. We observe that the theoretical value of the acceleration parameter $a_0 = 5.4\times10^{-10}\,\mathrm{m/s^2}$ (blue line reference in Figure 4) is consistent at 2-σ level for all galaxies. Moreover, it is worth noticing that all galaxies show a strong degeneracy between the acceleration parameter and the stellar mass-to-light ratio. In particular Fornax exhibits a bimodality, see Figure 4, but all galaxies are now consistent with $\Upsilon_* < 6$. This strong degeneracy may drive Υ_* to lower values, hence observationally preferred, by increasing the value of a_0 from the theoretical one. As we mentioned before, this could be allowed by the model as we do not know the real deformation pattern of the elastic medium by the presence of the dSph galaxies.

We have also corroborated the prediction we made at

the beginning of this section for the difference between Verlinde's and MOND mass-to-light ratio required for each model to fit the data. This was verified numerically by performing the fits as described in this section, for the same Plummer profile, but with the mass profile determined by MOND theory and with fixed acceleration parameter a_0. A different analysis for the dSph's kinematics within MOND was made in Ref. [33], where different key assumptions were made. In particular, the author considered a King profile with an anisotropic function β which is not constant but linear in the radial variable. While the density profile may not change drastically from our analysis, the non-constant β could hide deviations in the mass-to-light ratio with respect to our fittings. However, even after considering these issues, the author of [33] finds higher mass-to-light ratios than ours, where only two cases have $\Upsilon_* < 3$, in agreement with the expected result of a higher values than in Verlinde's proposal, as we have argued here. Finally, we do not attempt to scrutinize the details of both studies, since we believe comparing Verlinde's model to MOND should be a carried under the same assumptions, as we have done here.

V. DISCUSSION

In this paper we have explored the consequences of a model that proposes that spacetime emerges as the result of the entanglement structure of an underlying microscopic theory. However, apart from some sketches of how it may look like, there is not such a concrete construction of the microscopic theory. Driven by arguments, Erick Verlinde has recently argued that an effective theory can capture the key ingredients of the relevant microscopic degrees of freedom to describe the DM phenomena [8]. This effective model is simply the theory of linear elasticity, where the DM component appears as a memory effect of the medium due to the presence of the standard model of particles. At this level, one may even forget about the microscopic derivation, and consider the elastic theory as the concrete proposal behind DM.

For spherically symmetric isolated massive objects, and assuming further an elastic-medium response of maximal deformation, Verlinde identifies the expression in Eq. (6) as codifying the correction to the the baryonic mass profile $M_B(r)$ for the observed gravitational field, $M(r) = M_B(r) + M_D(r)$. Outside the mass, we can simply look at this theory as a particular realization of MOND. We identify that in the exterior limit the deviation of Verlinde's theory with respect to the recently proposed interpolation function of McGaugh *et al* [5] is never larger than 30 percent, marginally accepted by their observations.

However, within the interior part of a massive object, the gravitational field clearly departs from that of MOND. The key difference is that Verlinde's interpolating function contains a radial derivative of the mass profile. Therefore, only a very particular mass profile in Verlinde's theory will reduce to McGaugh's interpolation formula. None of the common density models used to describe galaxies in a cosmological framework is expected to be such a special case. In particular, for a Plummer density profile one finds up to a 50 percent relative difference with respect to the external region in the interior of dSph galaxies.

One should never forget that Physics is an experimental discipline, and only observations can decide if a model is correct or not. By following this line of thought, in this paper we just took the expression in Eq. (6) for the spherically symmetric apparent mass distribution for granted, and show that this effective model can describe the internal kinematics of the eight classical dSph satellites of the Milky Way without postulating any kind of dark component. In the analysis we found a degeneracy between the acceleration parameter, a_0, and the mass-to-light ratio, Υ_*, which drives Υ_* to values larger than expected as we approach the theoretical value of $a_0 = cH_0$.

If one considers Eq. (6) as a phenomenological model to describe DM, and forgets about the elastic medium, the derivation assumptions, or the microstates motivation, then one could argue that Verlinde's proposal has a mild tension in the fittings, as we have shown in our Table I, test 1, due to the marginally unacceptable high values of Υ_*. However, once we get back to the assumptions of the elastic medium, we find that a maximal deformation was considered. By relaxing this condition, which is encoded in Eq. (5), the acceleration scale a_0 as free parameter can capture the information about the non-maximal deformation of the elastic medium, which will translate on a larger value than the theoretical one, due to the inequality sign of (5), and in agreement with our findings. Other astrophysical and modeling systematics could be getting into preferring a higher value of a_0 than cH_0, but this is beyond our present expectations [37]. It is important to say that we have not, in any sense, confronted this hypothesis against the standard DM one.

In order to improve future analysis of the study presented here, it is important to stress the nature of all the different assumptions made within this work. We considered that dSph galaxies can be described as isolated objects with spherical symmetry. Of course these systems are not really isolated, due to their proximity to the Milky Way. We have compared the values of the exterior gravitational field due to the Milky Way, $g_{\rm MW}$, to that of Verlinde's model, g. In order to estimate $g_{\rm MW}$ one would need the complete theory, but we can argue that $g_{\rm MW} \lesssim (170\,{\rm km/s})^2/R_{\rm MW}$, where the upper bound represents the terminal velocity of objects orbiting in the Milky Way in the galactic plane at a distance $R_{\rm MW}$ to the center of the galaxy. In Table I we report the ratio $g_{\rm MW}/g$, with $g \sim (a_0 G \Upsilon_* L_V)^{1/2}/r_{\rm half}$, and find that it is always (apart from Sextans, which does not pose any other problem) negligible at the level of the precision obtained by our fittings. On the other hand, these spheroidal systems are not really spherical, but they are

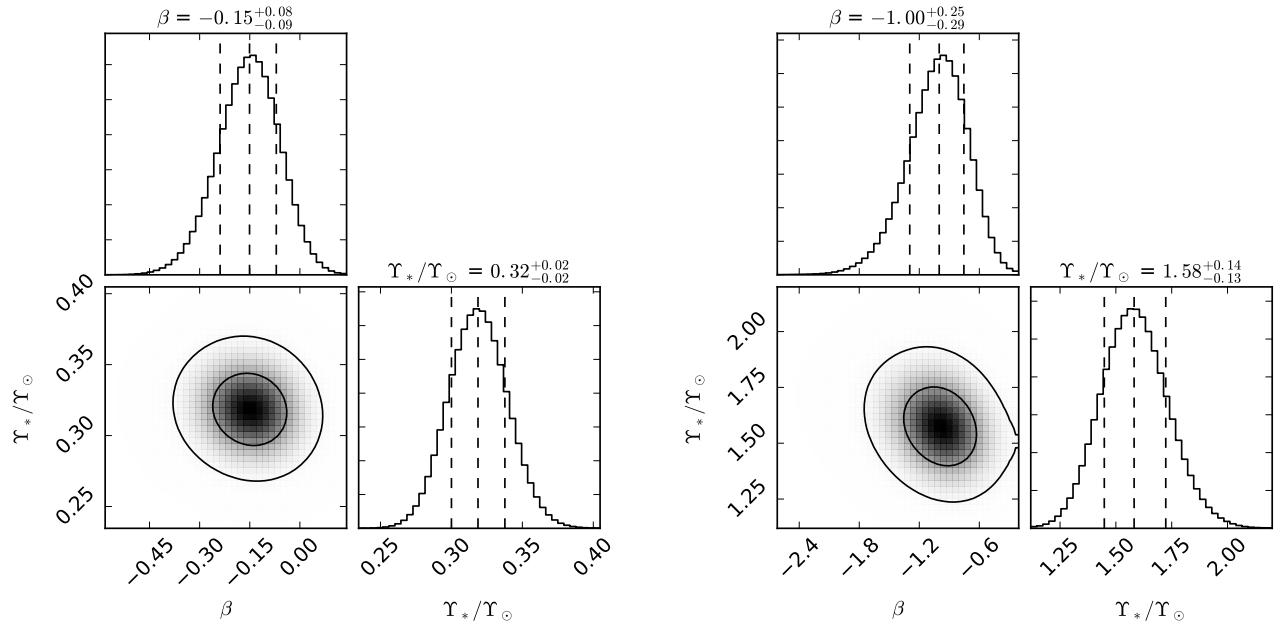

FIG. 3: *Test 1:* Posterior distribution function of the anisotropy β, and stellar mass-to-light ratio Υ_*, in Fornax (left), and Sculptor (right), as resulted from the fit to their velocity dispersion profile under Verlinde's theory, assuming a constant $a_0 = 5.4 \times 10^{-10}\,\mathrm{m/s^{-2}}$. Both parameters are well constrained and show no degeneracy between them. The other galaxies show similar results.

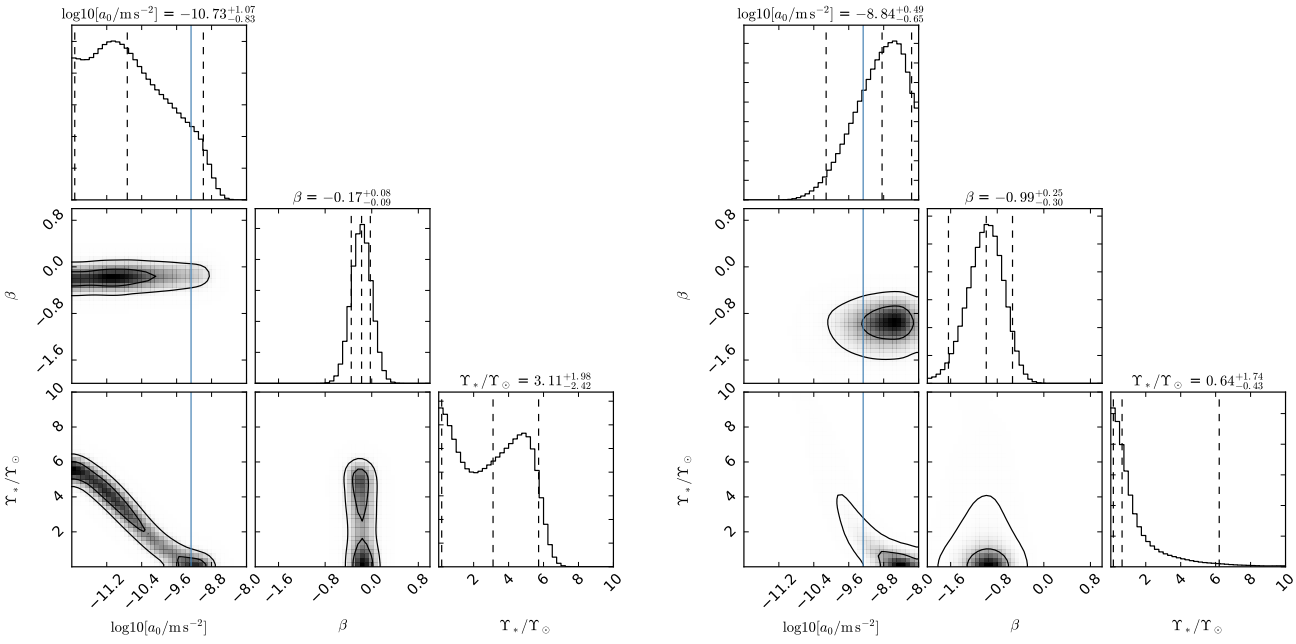

FIG. 4: *Test 2:* Posterior distribution function of the anisotropy β, stellar mass-to-light ratio Υ_*, and acceleration scale a_0, in Fornax (left), and Sculptor (right), as resulted from the fit to their velocity dispersion profile under Verlinde's theory. Here we consider the parameter a_0 to be free. As before in test 1, β and Υ_* show no correlation between them. However, there is a strong degeneracy between a_0 and Υ_*, which is more evident for Fornax, where the Υ_* posterior is bimodal. This degeneracy is present in all other galaxies, similar to the banana shape of the Υ_*-a_0 posterior distribution for Sculptor. For reference, the blue line represents the theoretical value of the acceleration scale at $a_0 = 5.4 \times 10^{-10}\,\mathrm{m/s^{-2}}$. This value is consistent at 2-σ level for all galaxies.

the highly DM-dominated objects for which such an assumption is best justified, since the radial averaged ellipticity for the for the eight galaxies is $\epsilon_{avg} = 0.05$, with a maximum of $\epsilon_{max} \sim 0.3$ (except for UMi that is $\epsilon = 0.56$) [30].

To conclude, we have shown how Verlinde's emergent gravity model and MOND predict very different relations in the g vs g_B plane for spherically symmetric configurations, which may help discriminate between both proposals. In particular, we have studied in detail the inner configuration of dSph satellites of the Milky Way. However, more precision in both, stellar kinematics and mass-to-light ratio, are required in order to favor one model over the other at the dSph's scales. As well more theoretical work is needed so that one can consider non-spherically symmetric objects.

Acknowledgments

We are grateful to Matthew Walker for providing us with the observational data. We are also grateful to Nana Cabo, Oscar Loaiza, Octavio Obregón, Jorge Peñarrubia, and Miguel Sabido for useful discussions and/or reading the manuscript. AXGM acknowledges support from Cátedras CONACYT and UCMEXUS-CONACYT collaborative project funding. This work is supported by CONACyT-Mexico grants 182445, 167335, 179208, 179881 and Fronteras de la Ciencia 281, and also by DAIP-Universidad de Guanajuato grants 1,046/2016 and 878/2016 .

Appendix A: Apparent DM masses in different regimes

The mass distribution of baryons in a dSph can be read from the standard formula $M_B(r) = 4\pi \int_0^r \nu(r') r'^2 dr'$, once the stellar mass density profile $\nu(r)$ is specified. For the case of a Plummer profile (8) the apparent DM mass in Verlinde's theory, $M_D(r)$ from Eq. (6), is then given by

$$M_D(x) = \frac{\mathcal{N}_0 x^{5/2}}{(1+x^2)^{3/4}} \sqrt{\frac{4+x^2}{1+x^2}}\,, \tag{A1}$$

where $x = r/r_{\rm half}$, and

$$\mathcal{N}_0 = (L r_{\rm half}^2 \Upsilon_*)^{1/2} \sqrt{\frac{a_0}{6\,G}}\,. \tag{A2}$$

Notice that the first (second) term in $\mathcal{N}_0$ is observationally (theoretically) defined. For comparison we also give the corresponding apparent DM mass in the extreme MOND regime, namely

$$M_D(x) = \frac{\mathcal{N}_M x^{5/2}}{(1+x^2)^{3/4}}\,, \tag{A3}$$

where this expression has also been obtained using a Plummer profile. Here $\mathcal{N}_M$ is equal to the expression in Eq. ($A2$) but replacing $a_0 \to 6a_M$. From equations (A1) and (A3), the difference between Verlinde's theory and MOND apparent DM masses is $\sqrt{(4+x^2)/(1+x^2)}$, which gives a factor of $\sqrt{5/2}$ when evaluated at $x = 1$. Note that in both cases one can get the same value for the apparent DM mass contained at the half-light radius if the stellar mass-to-light ratio is 5/2 times greater in the case of MOND than in Verlinde. It is then natural to understand why Verlinde's emergent gravity proposal points to lower values of Υ_* than MOND.

[1] S. Profumo, *An Introduction to Particle Dark Matter,* World Scientific (UK, November 30, 2016) 250pp

[2] V. Vitale and A. Morselli for the Fermi/LAT Collaboration, "Indirect search for dark matter from the center of the Milky Way with the Fermi-Large Area Telescope," Proceedings of the 2009 Fermi Symposium (2009) [arXiv:0912.3828]; R. Bernabei *et al.*, "DAMA results at Gran Sasso underground lab," Nucl. Part. Phys. Proc. **87** 263-264 (2015); R.D. Parsons *et al* for the H.E.S.S. Collaboration, "Sgr A* observations with H.E.S.S. II," Proceedings of the 34th International Cosmic Ray Conference (2015) [arXiv:1509.03425]

[3] M. Milgrom, "A modification of the Newtonian dynamics as a possible alternative to the hidden mass hypothesis," Astrophys. J **270** 365370 (1983); M. Milgrom, "A modification of the Newtonian dynamics: Implications for galaxies," Astrophys. J **270** 371389 (1983); M. Milgrom, "A modification of the newtonian dynamics: Implications for galaxy systems," Astrophys. J **270** 384 (1983)

[4] B. Famaey and S.S. McGaugh, "Modified Newtonian Dynamics (MOND): Observational phenomenology and relativistic Extensions," Living Rev. Relativity **15** 19 (2012) [arXiv:1112.3960]

[5] S. McGaugh, F. Lelli and J. Schombert, "The radial acceleration relation in rotationally supported galaxies," Phys. Rev. Lett. **117** 201101 (2016) [arXiv:1609.05917]

[6] E. Pointecouteau and J. Silk, "New constraints on MOND from galaxy clusters," Mon. Not. Roy. Astron. Soc. **364** 654 (2005) [astro-ph/0505017]; R.H. Sanders, "Clusters of galaxies with modified Newtonian dynamics (MOND)," Mon. Not. Roy. Astron. Soc. **342** 901 (2003) [astro-ph/0212293]

[7] M. Milgrom, "The modified dynamics as a vacuum effect," Phys. Lett. A **253** 273 (1999) [astro-ph/9805346]

[8] Erik Verlinde, "Emergent gravity and the dark universe," (2016) [arXiv:1611.02269]

[9] Akbar Salam, *Non-relativistic QED theory of the Van der Waals dispersion interaction,* Springer International Publishing (2016) 105pp

[10] J.A. Wheeler in *Relativity, Groups, and Topology*, Edited by B.S. DeWitt and C. DeWitt, Gordon and Breach (New York, 1964), 929 pp.; D. Finkelstein, "Space-Time code," Phys. Rev. **184** 1261 (1969)

[11] A.D. Sakharov, "Vacuum quantum fluctuations in curved space and the theory of gravitation," Dokl. Akad. Nauk **1** 70-71 (1967), reprinted in Gen. Rel. Grav. **32** 365-367 (2000)

[12] L. Sindoni, "Emergent models for gravity: an overview of microscopic models," SIGMA **8** 027 (2012) [arXiv:1110.0686]

[13] N. Seiberg, "Emergent spacetime," The Quantum Structure of Space and Time: Proceedings of the 23rd Solvay Conference on Physics (2006) [hep-th/0601234]; S. Carlip, "Challenges for emergent gravity," Stud. Hist. Phil. Sci. B **46** 200 (2014) [arXiv:1207.2504; T. Padmanabhan, "Gravity and spacetime: an emergent perspective," in Springer Handbook of Spacetime, pp 213-242 (2014)

[14] S. Weinberg and E. Witten, "Limits on massless particles," Phys. Lett. B **96** 59 (1980)

[15] T. Jacobson, "Thermodynamics of spacetime: The Einstein equation of state," Phys. Rev. Lett. **75** 12601263 (1995)

[16] T. Padmanabhan, "Thermodynamical aspects of gravity: new insights," Rept. Prog. Phys. **73** 046901 (2010) [arXiv:0911.5004]

[17] E.P. Verlinde, "On the origin of gravity and the laws of Newton," JHEP **1104** 029 (2011) [arXiv:1001.0785]

[18] J. Eisert, M. Cramer and M. B. Plenio, "Area laws for the entanglement entropy —a review," Rev. Mod. Phys. **82** 277 (2010) [arXiv:0808.3773]

[19] R. Orus, "A practical introduction to tensor networks: matrix product states and projected entangled pair states," Annals Phys. **349** 117 (2014) [arXiv:1306.2164]

[20] M. Nozaki, S. Ryu and T. Takayanagi, "Holographic geometry of entanglement renormalization in quantum field theories," JHEP **1210** 193 (2012) [arXiv:1208.3469]

[21] S. Ryu and T. Takayanagi, "Holographic derivation of entanglement entropy from AdS/CFT," Phys. Rev. Lett. **96** 181602 (2006) [hep-th/0603001]

[22] T. Padmanabhan, "Gravity as elasticity of spacetime: A Paradigm to understand horizon thermodynamics and cosmological constant," Int. J. Mod. Phys. D **13** 2293 (2004) [gr-qc/0408051]

[23] P.A.R. Ade *et al* [*Planck* Collaboration], "Planck 2015 results. XIII. Cosmological parameters," Astron. Astrophys. **594** A13 (2016) [arXiv:1502.01589]

[24] L.H. Liu and T. Prokopec, "Gravitational microlensing in Verlinde's emergent gravity," (2016) [arXiv:1612.00861]; M. M. Brouwer *et al.*, "First test of Verlinde's theory of Emergent Gravity using Weak Gravitational Lensing measurements," (2016) [arXiv:1612.03034]; L. Iorio, "Are we close to put the anomalous perihelion precessions from Verlinde's emergent gravity to the test?," (2016) [arXiv:1612.03783]

[25] E.F. Bell and R.S. de Jong, "Stellar mass-to-light ratios and the Tully-Fisher relation," Astrophys. J. **550** 212229 (2001)

[26] M. Walker in *Planets, Stars and Stellar Systems. Volume 5: Galactic Structure and Stellar Populations,* Springer Netherlands (2013) 1039pp

[27] M.G. Walker, M. Mateo, E.W. Olszewski, J. Peñarrubia, N.W. Evans and G. Gilmore, "A universal mass profile for dwarf spheroidal galaxies," Astrophys. J. **704** 1274-1287 (2009) [arXiv:0906.0341[astro-ph.CO]]; Erratum-ibid. **710** 886-890 (2010)

[28] M.G. Walker, M. Mateo, E.W. Olszewski, O.Y. Gnedin, X. Wang, B. Sen and M. Woodroofe, "Velocity dispersion profiles of seven dwarf spheroidal galaxies," Astrophys. J. **667** L53-L56 (2007) [arXiv:0708.0010[astro-ph]]

[29] J. Peñarrubia, J.F. Navarro, A.W. McConnachie and N.F. Martin, "The signature of galactic tides in Local Group dwarf spheroidals," Astrophys. J. **698** 222 (2009) [arXiv:0811.1579]

[30] A.W. McConnachie, "The observed properties of dwarf galaxies in and around the Local Group" Astrophys. J. **144** 4 (2012)

[31] J. Binney and S. Tremaine, *Galactic Dynamics,* Princeton University Press, Second Edition (27 de enero de 2008) 904pp

[32] D. Foreman-Mackey, D.W. Hogg, D. Lang and J. Goodman, "emcee: The MCMC Hammer," Publications of the Astronomical Society of the Pacific **125** 306-312 (2013) [arXiv:1202.3665]

[33] G.W. Angus, "Dwarf spheroidals in MOND," Mon. Not. Roy. Astron. Soc. **387** 1481 (2008) [arXiv:0804.3812]

[34] E.N. Kirby, J.G. Cohen, P. Guhathakurta, L. Cheng, J.S. Bullock and A. Gallazzi, "The universal stellar mass-stellar metallicity relation for dwarf galaxies," Astrophys. J. **779** 102 (2013) [arXiv:1310.0814]

[35] J. Woo, S. Courteau, and A. Dekel, MNRAS **390** 1453 (2008)

[36] H.C. Plummer, "On the problem of distribution in globular star clusters," Mon. Not. R. Astron. Soc. **71** 460 (1911)

[37] A. X. Gonzales-Morales, D. J. E. Marsh, J. Peñarrubia and L. Urena-Lopez, (2016) [arXiv:1609.05856]